03.4

Rivulet interaction on surfaces of heated liquid films

© E.A. Chinnov, V.V. Semionov

Kutateladze Institute of Thermophysics, Siberian Branch, Russian Academy of Sciences, Novosibirsk, Russia
E-mail: vitalik.semionov@gmail.com

Received August 16, 2022
Revised October 7, 2022
Accepted October 11, 2022

Study of the water film flow along the vertical heater at Reynolds number Re = 33 and initial temperature $T_0 = 23^\circ$C was carried out. Some types of interaction between rivulets on the surface of a heated liquid film were distinguished. It is shown that thermocapillary structures appearance in the heater upper part leads to rivulets deflection and interaction.

Keywords: liquid film, thermocapillary instability, regular structures.

DOI: 10.21883/TPL.2022.12.54938.19343

Films flowing down by gravity are widely used in various industrial machines and setups: low−pressure evaporators used in food products concentration and production of pharmaceuticals, seawater desalination plants, and rectification columns. Film flows are employed in cooling systems, chemical technologies, etc. To design and implement those devices, it is important to understand the processes taking place in heated liquid films.

Two−dimensional (2D) hydrodynamic waves in isothermal liquid films are unstable to three−dimensional (3D) perturbations. The wavelength of instability to transverse 3D perturbations decreases with increasing Reynolds number [1]. It has been found out that the transition from regular 2D structures to the 3D flow is accompanied by essential longitudinal redistribution of the liquid [2,3]. Characteristic forms of 3D structures evolving during the transition were described. The rivulet formation mechanism was discussed in [3]: when the 3D wave passes along the residual liquid film layer, there takes place a lateral suction (inleakage) of the liquid to under the wave crest and its discharge through a wake with an increased film thickness behind the wave. This wake behind the wave induces synchronization of the wave pattern: the waves align in chains thus making the liquid being sucked continuously to the same flow regions, which gives rise to rivulets.

While the liquid films flow over the heated surfaces, there arises not only hydrodynamic instability leading to the wave flow development, but also various−type thermocapillary instabilities associated with the liquid transfer along the phase interface because of formation of the surface tension gradient [4]. Regular structures of two types (A and B) were distinguished in the heated liquid film. Formation of a 3D regular structure (named later as structure A) in the film of a 25% aqueous alcohol solution flowing down over a plane with a small−size heater (6.5×13 mm) at low Reynolds numbers was for the first time revealed in experiments of [5]. Formation of thermocapillary structures in regime B in a heated liquid film with developed wave motion was studied in [6,7].

The natural evolution of developed 3D waves into thermocapillary rivulets during heating of the water film flowing down vertically under low temperature gradients was studied in [8] at Re = 10. A fact was fixed that horseshoe−shaped hydrodynamic waves undergo deformation in passing through the heated area. It was shown that, during the 3D wave propagation along the heater, temperature inhomogeneities emerged on the wave front, which led to the liquid film deformation and large waves' destruction due to the action of thermocapillary forces. It was established that thermocapillary forces also can transversely deflect mid−size 3D waves and parts of decayed large 3D waves thus promoting formation of jets in the form of vertical rivulets. Interaction between incoming waves with thermocapillary structures at Re = 50 was studied in [9].

In work [10], motion of rivulets across the film flow (deflection) was investigated. The maximal deflection amplitude was shown to exhibit a threshold increase with increasing heat flux density.

The goal of this work was to study various types of interaction between 3D waves and thermocapillary structures (touching, merging and branching (bifurcation)) at Reynolds number Re = 33 and film initial temperature $T_0 = 23^\circ$C.

The setup was designed as a closed circulation loop comprising a reservoir with a pump, working section, filter, rotameters, pipelines, and shutoff valves. The working section consisted of a base plate with a film former, temperature stabilizer and heater mounted on it. The fluid (water with dye) was pumped to the film former that consisted of an accumulation chamber, distributor, and nozzle with a calibrated flat slot. The liquid flowed down along the plate and returned by gravity to the reservoir with the electric pump through connecting channels. As the heating element, a flat copper heat−exchanger 150 mm wide and 100 mm long was used, through which hot water was pumped. The experiments were performed

at Reynolds number $\mathrm{Re} = 33$ ($\mathrm{Re} = W/\rho\nu$, where W is the specific mass flowrate of the liquid, ρ is the liquid density, ν is the kinematic viscosity coefficient of the liquid.

Surface temperature of the vertically falling liquid film and its thickness distribution in the heater area were measured synchronously. The experiments employed an infrared scanner Titanium HD 570M able to measure the temperature field on the film surface with resolution of up to 640×512 pixels, full frame frequency of up to 115 Hz, and sensitivity of 18 mK. To determine the instantaneous film thickness field, a modified fluorescent method was used. The fluorophore excitation was performed by using a laser uninterruptedly illuminating a 120×120 mm area. Light reradiated by the fluorophore was registered by a digital camera. In front of the camera there was installed a red filter used to cut off the reflected laser light. Measurements of the thickness and temperature fields were synchronized with the aide of a light signal. Detailed description of the experimental setup and procedure is given in [9].

Interaction between the waves and thermocapillary structures results in formation of rivulets on the liquid film surface, their motion across the flow (deflection), and interaction with each other (Fig. 1). Hereinafter the vertical arrows indicate the flow direction.

As a characteristic of the rivulets' transverse motion, the maximal deflection amplitude (A_r) was used which is the distance between the extreme right and extreme left rivulet positions during a time interval multiple of that of the wave passage along the heater. To calculate the rivulet deflection amplitude, instantaneous temperature profiles in the flow cross–section (in the Z direction) were analyzed. The temperature profiles were processed at two points on the X axis that is parallel to the film flow ($X = 50$ and 75 mm from the heater top edge). Temperature minima corresponding to instantaneous positions of the rivulet crest were determined for each instantaneous profile.

Several types of rivulet interaction were distinguished: type 0 is the absence of interaction, when the wave propagating along the rivulet crest reaches the heater end without interaction with other rivulets; type 1 is merging of two rivulets into one (Fig. 2, *a*); type 2 is the bridge, when the rivulets merge and then separate (Fig. 2, *b*); type 3 is rivulet branching, when a rivulet gets divided into two (Fig. 2, *c*).

The numbers of each–type interactions were counted at different heat fluxes, both in the absence of structures A and pronounced zigzag motion of rivulets (deflection) and in their presence. To prevent the influence of finiteness of heater dimensions, interaction of only five rivulets in the center of the heater were taken into account.

All the 600 frames made by a thermal camera were examined in turn, all the interactions of types 1, 2 and 3 were fixed. As the type 0 interaction, there were considered

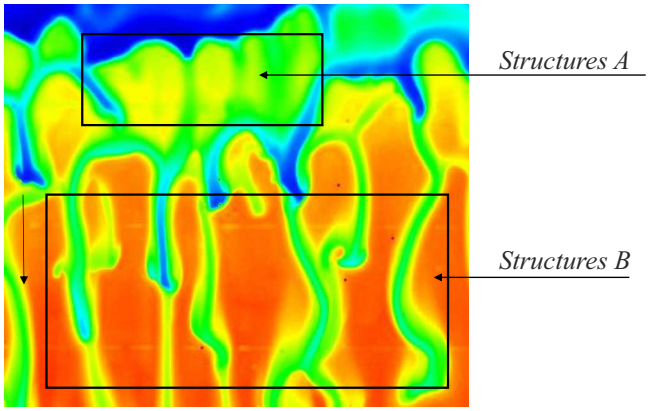

Figure 1. Instantaneous temperature distribution on the film surface in the heater central part (69×60 mm in area) at $\mathrm{Re} = 33$. The film initial temperature is $T_0 = 23^\circ$C, $q = 4.15$ W/cm^2.

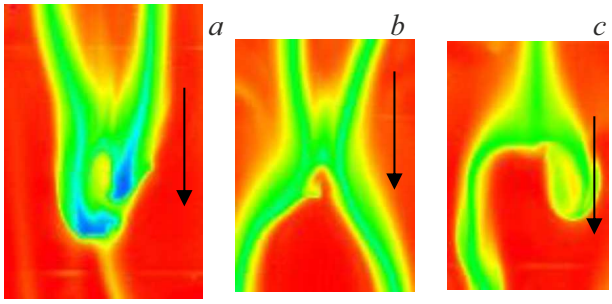

Figure 2. Different types of the rivulet interaction.

rivulet–surface waves propagating into the region under consideration without interactions.

Then the number of each–type interactions was divided by the sum of all interactions; thus, the fractions of interactions of each type were determined. Based on the obtained results, histograms were constructed.

Fig. 3 presents the dependence of maximal amplitude of the zigzag rivulet motion on the heat flux for two different distances from the heater top edge, and distribution histograms for different–type interactions for certain heat fluxes. Once the heat fluxes corresponding to the thermocapillary structure A formation in the heater top part are reached, a threshold increase in the maximal amplitude of the rivulet zigzag motion takes place, as well as significant changes in the distribution of interactions by types: the fraction of the type–0 interaction decreases, while those of types 1–3 increase.

Thus, we have shown that development of the thermocapillary instability in the top part of the heater results in an increase in the rivulet zigzag motion amplitude. Maximal amplitudes of the rivulet deflection are observed at high heat fluxes corresponding to formation of thermocapillary structures in regime A. Interaction of rivulets in a heated liquid film has been described and analyzed for the first time; different types of interaction

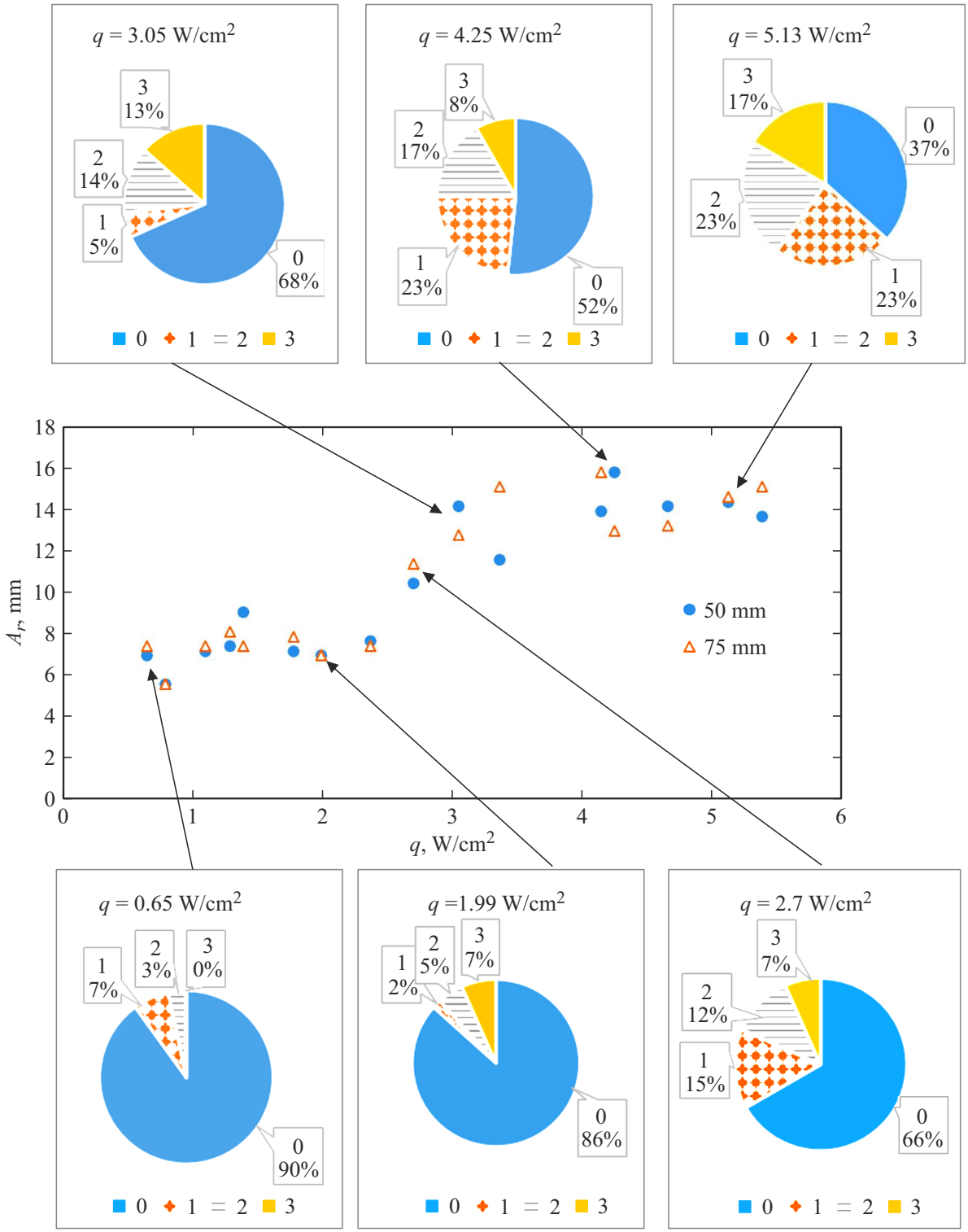

Figure 3. Dependence of the maximal deflection amplitude on the heat flux for two distances from the heater upper edge (50 and 75 mm), and distribution histograms for different interaction types.

have been distinguished. We have established that the increase in the rivulet zigzag displacement amplitude causes the rivulet interaction (touching, merging and branching (bifurcation)).

Motion and interaction of the rivulets contributes preventing dry spots formation on the heater surface, rewetting of dried areas, and, finally, enhancement of the critical heat flux corresponding to the liquid film rupture.

Financial support

The study was supported by the Russian Scientific Foundation (Project 22-19-20090) and Novosibirsk Region Government (Contract № r-13).

Conflict of interests

The authors declare that they have no conflict of interests.

References

[1] C.D. Park, T. Nosoko, AIChE J., **49** (11), 2715 (2003). DOI: 10.1002/aic.690491105
[2] S.V. Alekseenko, V.V. Guzanov, D.M. Markovich, S.M. Kharlamov, Tech. Phys. Lett., **38** (8), 739 (2012). DOI: 10.1134/S1063785012080159.
[3] S.V. Alekseenko, A.V. Bobylev, V.V. Guzanov, D.M. Markovich, S.M. Kharlamov, Tech. Phys. Lett., **40** (11), 1031 (2014). DOI: 10.1134/S1063785014110170.
[4] E.A. Chinnov, O.A. Kabov, J. Appl. Mech. Tech. Phys., **44** (5), 708 (2003). DOI: 10.1023/A:1025564605979.
[5] O.A. Kabov, v sb. *Ros. nats. konf. po teploobmenu* (Izd. dom MEI, M., 1994), t. 6, s. 90–95. (in Russian)
[6] E.A. Chinnov, A.D. Nazarov, A.V. Saprykina, A.F. Serov, Thermophys. Aeromech., **14** (1), 67 (2007). DOI: 10.1134/S086986430701009X.
[7] V.V. Lel, A. Kellermann, G. Dietze, R. Kneer, A.N. Pavlenko, Exp. Fluids, **44** (2), 341 (2008). DOI: 10.1007/S00348-007-0408-X
[8] E.A. Chinnov, E.N. Shatskii, Tech. Phys. Lett., **42** (10), 997 (2016). DOI: 10.1134/S1063785016100047.
[9] E.A. Chinnov, Int. J. Heat Mass Transfer, **108** (Pt B), 2053 (2017). DOI: 10.1016/j.ijheatmasstransfer.2017.01.070
[10] V.V. Semionov, E.N. Shatskiy, E.A. Chinnov, J. Phys.: Conf. Ser., **1105**, 012074 (2018). DOI: 10.1088/1742-6596/1105/1/012074